SANDIA REPORT SAND82-0631 • Revised • Unlimited Release
Printed June 1983
Reprinted September 1983

Modal Testing of a Rotating Wind Turbine

Thomas G. Carne, Arlo R. Nord

Prepared by
Sandia National Laboratories
Albuquerque, New Mexico 87185 and Livermore, California 94550
for the United States Department of Energy
under Contract DE-AC04-76DP00789

Supersedes SAND82-0631 Dated November 1982

Issued by Sandia National Laboratories, operated for the United States Department of Energy by Sandia Corporation.

Printed in the United States of America
Available from
National Technical Information Service
U.S. Department of Commerce
5285 Port Royal Road
Springfield, VA 22161

NTIS price codes
Printed copy: A02
Microfiche copy: A01

SAND82–0631 Revised
Unlimited Release
Printed June 1983

Modal Testing of a Rotating Wind Turbine

Thomas G. Carne
Arlo R. Nord
Vibration and Modal Testing Division 7542
Sandia National Laboratories
Albuquerque, NM 87185

Abstract

A testing technique has been developed to measure the modes of vibration of a rotating vertical axis wind turbine. This technique has been applied to the Sandia 2-m turbine, where the changes in individual modal frequencies as a function of the rotational speed have been tracked from 0 rpm (parked) to 600 rpm. During rotational testing, the structural response was measured using a combination of strain gages and accelerometers, passing the signals through slip rings. Excitation of the turbine structure was provided by a scheme that suddenly released a pretensioned cable, thus plucking the turbine as it was rotating at a set speed. In addition to calculating the real modes of the parked turbine, the modes of the rotating turbine were also determined at several rotational speeds. The modes of the rotating system proved to be complex because of centrifugal and Coriolis effects. The modal data for the parked turbine were used to update a finite element model. Also, the measured modal parameters for the rotating turbine were compared to the analytical results, thus verifying the analytical procedures used to incorporate the effects of the rotating coordinate system.

Acknowledgments

The authors wish to acknowledge W. N. Sullivan's impetus to do the rotating modal test. C. M. Grassham made invaluable contributions in the design of the snap-release device and in the planning and maintenance of the signal processing system. Others who made significant contributions in the testing and data reduction are R. A. Watson, P. H. Adams, B. K. Cloer, and M. R. Weber.

Contents

Figures

Tables

Modal Testing of a Rotating Wind Turbine

Introduction

Wind turbines have received attention as a possible device for producing electric power from a renewable energy source. In general there are two types of wind turbines currently involved in major development programs. The horizontal axis (or propeller) turbine and the vertical axis turbine. Figure 1 shows the Sandia 17-m turbine, an example of a vertical axis wind turbine, which is the subject of this work. When the turbine is operating, both the tower and the blades rotate at a constant speed; the aerodynamic forces which are applied to the blades are transmitted through the tower as a torque to the electric generator. Since the orientation of the blades in the wind repeats itself at the constant rotation speed, the aerodynamic forces are periodic. These forces then have large spectral components at integral multiples of the rotation speed. There are broad band random forces caused by wind variability, but these are generally small compared to the discrete frequency forces. Because of the discrete frequency nature of this applied force, it is of paramount importance to understand the complete modal vibration characteristics of a turbine design so that operating the machine at a resonant frequency is avoided. Understanding the modal parameters is complicated since the frequencies, damping, and mode shapes are functions of the rotation speed and may vary over a wide range. Consequently, determining the modal characteristics of a parked turbine is *not* sufficient; it is necessary to know how the parameters have shifted at the proposed operating speed of the turbine.

This paper describes a technique for identifying the modal parameters of a *rotating* turbine and emphasizes the experimental details of work described in Reference 1. There were two objectives for developing this modal testing capability: (1) experimental data on representative hardware were required to verify the accuracy of an analysis technique based on finite element theory, and (2) a need existed for an established experimental technique for the measurement of rotating modal frequencies.

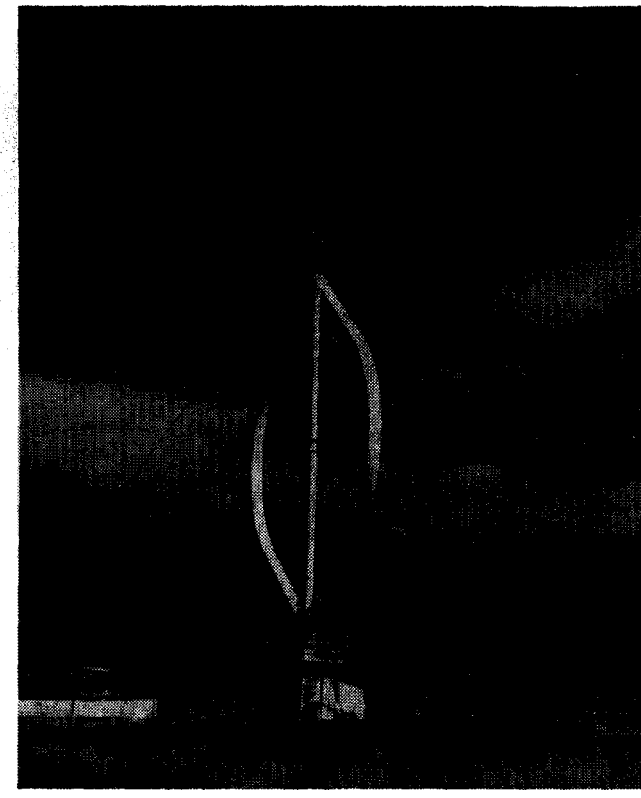

Figure 1. The Sandia 17-m Vertical Axis Wind Turbine

Correct identification of modal parameters using experimental data is a challenging task for any structure. It is further complicated for a rotating structure because (1) a mechanism must be devised to excite the structure while it is rotating; (2) the response data must be transmitted from the rotating system by means of slip rings or telemetry; and (3) unless the system can be tested in an evacuated chamber, aerodynamic excitation will cause undesired responses at integral multiples of the rotation speed.

Manufacturers of rotating structures (including helicopters, gas and steam turbines, rotary saws, computer disks, and wind turbines) have been interested in predicting the modal parameters of their structures. This interest is evidenced by the large number of papers that discuss analytical procedures for predicting modal parameters during rotation. References 2 through 10 are representative of some of the analytical approaches; Reference 1 briefly describes these techniques.

Reported analytical studies greatly outnumber experimental investigations. This is partly the result of previously mentioned experimental difficulties. Reference 11 discusses measuring the modes of a rotating model propeller blade by means of electromagnetic excitation. The test was performed in an evacuated chamber to reduce aerodynamic forces. A technique using small piezoelectric crystals as excitation devices, with an application to turbine blades, is reported in References 12 and 13; the crystals are driven by an applied voltage passed through slip rings. Reference 14 describes excitation by piezoelectric crystals with application to rotating saw blades. Saw blades are also examined in Reference 15, but a stationary electromagnet is used for excitation and a stationary, noncontacting displacement transducer is used for response measurements.

Use of either stationary excitation or stationary response transducers creates problems since both the excitation frequencies and the response measurements are explicitly dependent on rotation speed. The excitation force reported in Reference 16 partially avoids this difficulty using stationary air jets to excite turbine blades. In this application, blade frequencies were much higher than rotational frequencies, and the sixth multiple of the rotation frequency was used for excitation. Consequently, the problem of blade frequencies shifting rapidly with the changing rotation frequency was avoided. An evacuated chamber was used to reduce the other aerodynamic input, and a very small air gap between the air jet and the turbine disk was also required. Reference 17 describes a similar technique applied to a steam turbine, using steam nozzles and a vacuum chamber.

In each investigation involving rotating transducers, slip rings transmitted the signals from the rotating system. Some use has been made of optical or holographic techniques in an attempt to measure the response without using rotating instrumentation. The rotational frequency must be removed from those signals, causing further difficulty. In Reference 18 a novel approach for applying the excitation force is described. A force is imposed at the top bearing of a vertical-axis wind turbine, using a leaf spring; then the spring and resulting force are rotated with a separate motor and speed controller. The objective was to simulate the operational aerodynamic forces and measure impedance rather than modal properties, but this type of excitation could also be used for a modal investigation. In many of these applications it was difficult to limit unwanted aerodynamic excitation of the bladed systems; consequently, evacuated test chambers were used. Evacuated chambers and other special test equipment used by these investigators are unsuitable for field or on-site testing.

All of these references have attempted to produce single frequency or sine excitation, measuring frequency response functions one point at a time. This method requires long test times, and modes can be missed completely if there is not sufficient frequency resolution. The modal frequencies were then determined by picking peaks from the frequency response functions. The peak-picking technique can have severe shortcomings if the modes are closely spaced or coupled. Also, modal damping factors can be difficult to measure directly from the frequency response functions for closely spaced modes.

This paper examines a new procedure for experimentally determining the modal parameters of a rotating wind turbine. The testing technique incorporates an excitation force that is applied by using an internal quick-release device that operates while the structure is rotating. This excitation concept has many distinct advantages. Large structures can be much more easily excited with a quick-release device than with piezoelectric crystals or gas jets. Further, the excitation device is field compatible, allowing testing to be done on site if the test items cannot be brought into a lab. Finally, the quick-release device will excite all frequencies simultaneously, so that all modes can be excited by a single input, eliminating the need for a swept-frequency excitation.

Because of its variable speed capability and its convenient size, the Sandia 2-m turbine was used for the tests. First, a detailed modal test of the parked turbine was required so that modal characteristics would be well understood before starting the rotating test. The resulting modal parameters were then used to update a finite element model of the parked turbine. After the parked test, modal testing continued

on the rotating turbine at rotation speeds from 100 to 600 rpm. Mode shape data, modal frequencies, and modal damping factors were extracted from the experimental data. These modal frequencies were compared to predictions from a finite element analysis in which the effects of the rotation were taken into account [1].*

Mathematic Model

When performing a modal analysis of a rotating structure, the motion is most conveniently measured relative to a coordinate system that is rotating with the structure. This permits the displacements to be small by eliminating the large rigid-body rotation. To accurately model a rotating vertical axis turbine, the effects induced by the rotation that include tension stiffening, and the centrifugal and Coriolis terms must be included.

The tension stiffening that primarily affects the blades is induced from the steady centrifugal and gravity forces. The centrifugal and Coriolis terms are a direct result of using a rotating coordinate system. The total acceleration can be represented in terms of the acceleration in the rotating coordinate system by:

$$\underset{\sim}{a} = \ddot{\underset{\sim}{u}} + 2\,\underset{\sim}{\Omega} \times \dot{\underset{\sim}{u}} + \underset{\sim}{\Omega} \times [\underset{\sim}{\Omega} \times (\underset{\sim}{r} + \underset{\sim}{u})] \quad , \qquad (1)$$

where

$\underset{\sim}{a}$ = the total acceleration vector, excluding gravitational acceleration

$\underset{\sim}{r}, \underset{\sim}{u}, \dot{\underset{\sim}{u}}, \ddot{\underset{\sim}{u}}$ = the original position, the displacement, velocity, and acceleration vectors, respectively, as observed in the rotating coordinate system

$\underset{\sim}{\Omega}$ = the fixed angular velocity vector of that system.

Using this expression for the acceleration in the equation of motion for a structure, the usual damping and stiffness matrices are altered. The resulting differential equations are represented by

$$M\,\ddot{\underset{\sim}{u}} + C\,\dot{\underset{\sim}{u}} + K\underset{\sim}{u} - S\underset{\sim}{u} = \underset{\sim}{F}_c + \underset{\sim}{F}_g \quad . \qquad (2)$$

*Numbers in brackets refer to references listed at the end of the paper.

Here M is the normal mass matrix; C is the skew-symmetric Coriolis matrix, resulting from the second term on the right side of Eq (1); K is usual structural stiffness matrix; S is the centrifugal softening matrix that comes from the variable portion (dependent on u) of the last term of Eq (1); F_c is a static load vector representing the steady centrifugal forces that also comes from the last term of Eq (1); and, F_g represents the gravitational force that is also steady because of the vertical axis of rotation. Here we have ignored the structural damping, so the C matrix is totally due to the Coriolis effects. To obtain the modes and frequencies of the turbine as observed in the rotating system, Eq (2) is reduced to the following form:

$$M\ddot{u} + C\dot{u} + (K + K_G - S)\,u = 0 \quad , \qquad (3)$$

where K_G is the geometric stiffness matrix resulting from the steady centrifugal and gravitational loads. Thus, the solutions correspond to small motions about a prestressed state.

To find the eigenvalues of the system of equation represented by Eq (3), it is more convenient to use state vectors. Hence, introducing the state vector

$$\underset{\sim}{v} = \begin{Bmatrix} \dot{\underset{\sim}{u}} \\ --- \\ \underset{\sim}{u} \end{Bmatrix} \quad , \qquad (4)$$

and the matrices

$$A = \begin{bmatrix} M & O \\ O & \hat{K} \end{bmatrix} \quad , \qquad B = \begin{bmatrix} C & \hat{K} \\ -\hat{K} & O \end{bmatrix} \quad , \qquad (5)$$

where

$$\hat{K} = K + K_G - S \quad ;$$

then Eq (3) can be written as

$$A\,\dot{\underset{\sim}{v}} + B\,\underset{\sim}{v} = 0 \quad . \qquad (6)$$

Here A is real symmetric, and B is real skew symmetric. Seeking a solution for Eq (6) in the form $\underset{\sim}{v}(t) = \underset{\sim}{\phi}\, e^{i\omega t}$, the resulting eigenvalue problem is

$$[B + i\omega A]\,\underset{\sim}{\phi} = 0 \quad . \qquad (7)$$

Defining $\underset{\sim}{\phi} = A^{-1/2}\,\underset{\sim}{x}$ (assuming that A is now positive definite), Eq (7) may be transformed into a standard eigenvalue form

$$[G - \omega\, I]\,\underset{\sim}{x} = 0 \quad , \qquad (8)$$

where

$$G = i A^{-1/2} B A^{-1/2} \quad .$$

Because of the skew-symmetry of the matrix B, the matrix G is Hermitian. Consequently, it can be shown [19] that the eigenvectors are, in general, complex; but the eigenvalues are real.* If structural damping is included, the system loses its Hermetian character and the eigenvalues as well as the eigenvectors are complex. For the present work, structural damping has been ignored because most vertical axis wind turbines are lightly damped.

*If A is not positive definite, then G is no longer Hermetian and the eigenvalues are not necessarily real. This condition can lead to instability.

The Hermitian character of the eigenvalue system has important ramifications to the rotating modal test. Even if the modes of the parked structure are perfectly real, the modes of the rotating structure will be complex.

The important role of the rotation speed also becomes apparent by examining Eq (3). The overall stiffness matrix $\hat{K}$ is dependent on the rotation speed through the K_G and S matrices. The modal frequencies can vary tremendously with the rotation speed (see Fig. 2). This figure shows the variation in the modal frequencies of 10 modes for the Sandia 2-m turbine, as predicted by the finite element analysis [1].

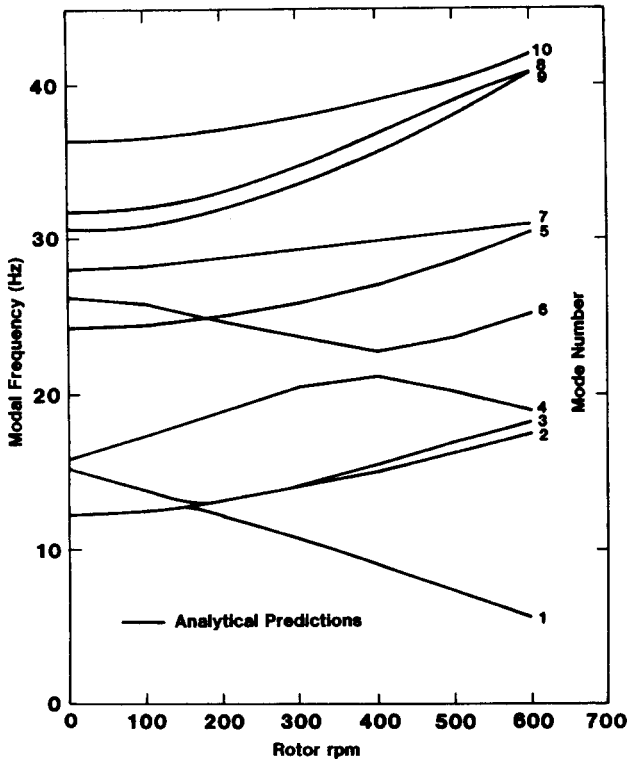

Figure 2. Predicted Variation in Modal Frequencies for the 2-m Turbine

Modal Testing of the Parked Turbine

We will present a brief overview of the general technique of modal testing with a minicomputer-based Fast Fourier Transform (FFT). The FFT technique, which involves exciting the structure with a force having a linear spectrum containing the frequency band of interest, is generally faster and more versatile than the classical swept-sine technique. The applied force and responses are measured in the time domain and transformed to the frequency domain using the FFT. The frequency response functions are then computed from the cross-spectral and auto-spectral densities of the applied force and the responses. Typically, several measurements are averaged to reduce the effects of uncorrelated noise. A more complete description of FFT modal testing is contained in Reference 20. The greater versatility of this technique is a result of more relaxed requirements on the excitation. For example, the technique is equally applicable to shaker-driven structures or structures excited by an instrumented hammer.

To develop and evaluate the modal testing technique for a rotating turbine, the Sandia 2-m turbine was chosen as the test vehicle because of its convenient size and variable speed capability. Fig. 3 shows some of its special features. The turbine is equipped with a motor and speed controller so that it can be operated in the absence of wind and at chosen speeds.

The parked modal test of the 2-m turbine actually consisted of two separate tests. In the first test, the turbine pedestal was supported on top of a 4-ft steel channel stand originally configured so that there would be more ground clearance for the blades. The stand was thought to be stiff compared to the turbine. However, it was later determined from the data that the stand contributed to much of the tower motion and greatly complicated the analytical model. After the modes were extracted from the data, two conclusions were drawn: (1) excessive base motion could cause complications in the understanding of the tower modes, and (2) the pedestal needed to be fully instrumented. A decision was made to remove the stand and retake the data. Some of the modal data reported here is from this first test, particularly that for the blade modes. Since their modes were not influenced by removing the base, the additional instrumentation on the blades in the first test provided a better representation of these mode shapes. The remainder of the parked modal data and all rotating data is from the second configuration with the stand removed and the pedestal attached directly to the concrete pad.

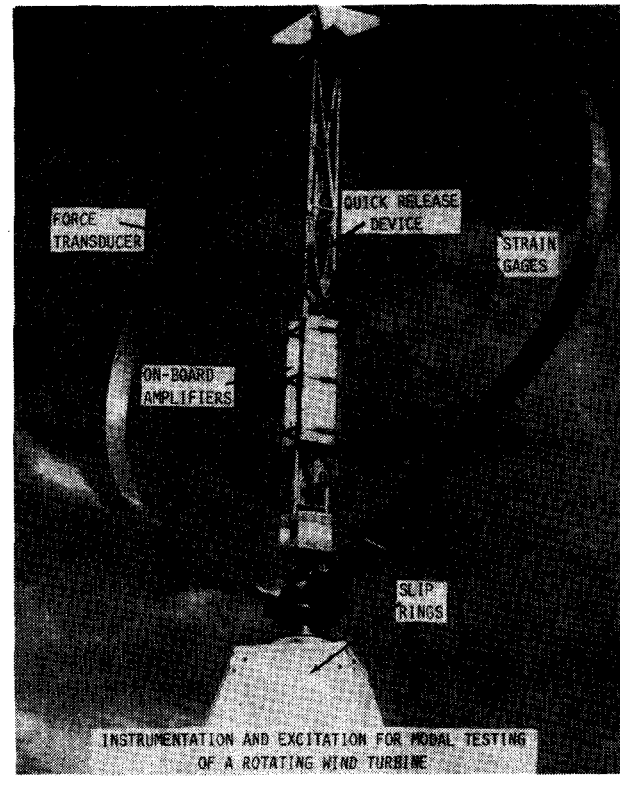

Figure 3. The Sandia 2-m Turbine With Instrumentation

The turbine was instrumented for the second parked test (Fig. 4) with 18 accelerometers on the blades, 10 on the tower, 20 on the pedestal, and 6 on the driveline. The structure was excited by striking the tower both in-plane and out-of-plane of the rotor at location 10; also by striking the blade flatwise and edgewise at location 6. Data taken from four different driving points gave assurance that all the tower and blade modes would be excited in at least one of the four test inputs.

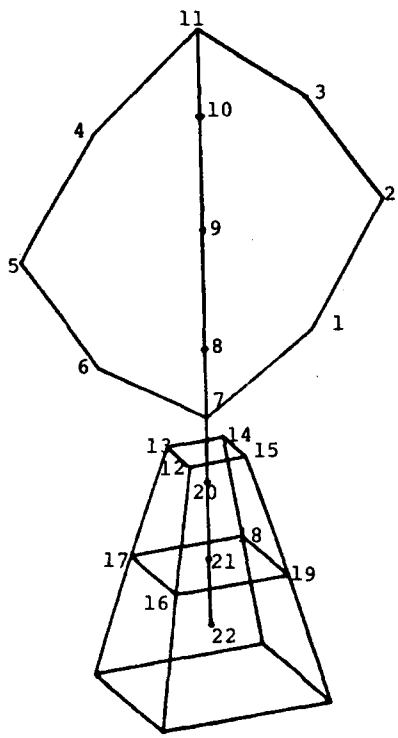

Figure 4. Measurement Locations for the Parked 2-m Turbine

Excitation for the parked modal test was provided by an instrumented 3-lb PCB hammer. The tip was selected to excite frequencies up to 60 Hz. All response monitoring for the parked tests was taken with Endevco 2221M2 piezoelectric accelerometers, conditioned through Endevco 2721B charge amplifiers. All input and response signals were low-passed at 100 Hz. They were amplified as necessary with Vishay 2310 signal conditioning amplifiers and recorded on an Ampex 2200 14-channel tape recorder.

Prior to the test, a two-channel analyzer had been used to determine the frequency range of interest, the resolution required, and the best locations for the driving points. From this procedure it was determined that all the modes of interest were between 10 and 60 Hz. The input force spectrum was tailored for this range, and the time histories were zoomed between its extremes to give a desirable frequency resolution (~0.1 Hz).

Fig. 5 shows a typical frequency response function derived from six samples of data with the magnitude plotted versus frequency. This response function is the response of a blade in the flatwise direction (perpendicular to the blade chord) resulting from a force input on the tower. The sharp resonant peaks clearly indicate modal frequencies and, because of their sharpness, corresponding low modal damping. Using additional minicomputer-based software [21] with a complete set of frequency response functions as input (one for each measurement point and direction), the modal frequencies, damping, and mode shapes were computed.

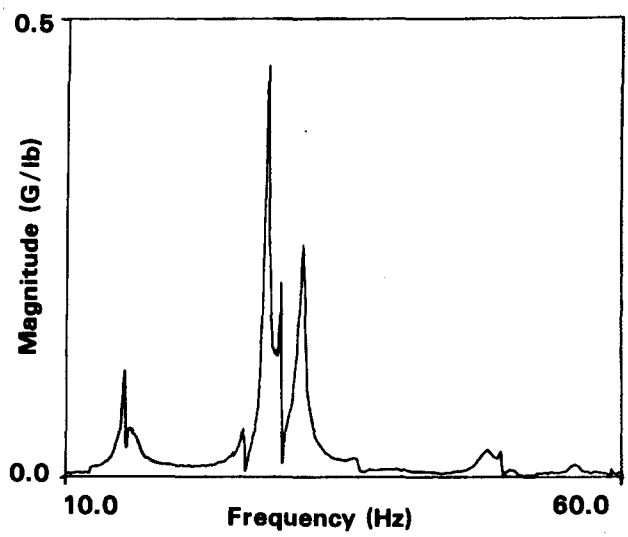

Figure 5. Typical Frequency Response Function From the Parked Modal Test

Table 1 shows the values of the modal frequency and damping for the lowest 14 modes with an identifying description of each mode. In conjunction with this table, Fig. 6 shows the three orthogonal views of each of these mode shapes, with the undeformed shape in solid lines and the deformed shape in dashed lines.

Table 1. Modal Frequencies and Damping Factors for the Parked Turbine

Mode No.	Mode Name	Measured Modal Frequency (Hz)	Measured Modal Damping (% of Critical)
1	1st antisymmetric flatwise	12.3	1.6
2	1st symmetric flatwise	12.5	1.6
3	1st rotor out-of-plane	15.3	0.7
4	1st rotor in-plane	15.8	0.7
5	Dumbbell	24.4	1.8
6	2nd rotor out-of-plane	26.2	0.5
7	2nd rotor in-plane	28.3	0.5
8	2nd symmetric flatwise	29.7	0.5
9	2nd antisymmetric flatwise	31.5	0.9
10	3rd rotor out-of-plane	36.5	1.1
11	3rd rotor in-plane	42.0	0.4
12	Pedestal mode	47.8	1.0
13	3rd antisymmetric flatwise	49.1	0.4
14	3rd symmetric flatwise	49.5	0.5

These modes were analyzed as real modes, so all the displacements are either in phase or out-of-phase with no phase shifts. Examining the first two modes of Fig. 6, one can see that they are a symmetric/antisymmetric pair of first flatwise blade modes. The next two modes (3 and 4) are the first two rotor modes, an out-of-plane and an in-plane. Mode 3 contains motion in both directions, while Mode 4 is purely in-plane. The fifth mode, a twisting of the rotor, appears shaped like a dumbbell from the side view. The sixth and seventh modes are the second rotor out-of-plane and in-plane modes, showing much greater blade deformations than the first rotor modes. Modes 8 and 9 are another pair of symmetric/antisymmetric blade modes. Modes 10 and 11 are the third pair of rotor modes. Examining the three rotor out-of-plane modes (3, 6, and 10), one can see some interesting comparisons by looking at the side views. In mode 3, the blades follow the tower with somewhat less deformation. For mode 6, the blades move in the same direction as the tower, but with an amplified motion. By contrast, in mode 10, the blades move in the opposite direction of the tower. Mode 12 is similar to the rotor in-plane modes, but with more motion coming from the base and drive train. Modes 13 and 14 are the third pair of symmetric/antisymmetric blade modes.

The primary purpose for this parked modal test was to understand the modes of the parked turbine and to use this information to evaluate the acurracy of the finite element model before using this model to predict modes of the rotating turbine. Table 2 compares the measured modes and the analytical modes for the first 10 modes both before and after modifying the model. From the data, it is easy to see the value of modal testing for correcting and tuning the finite element model.

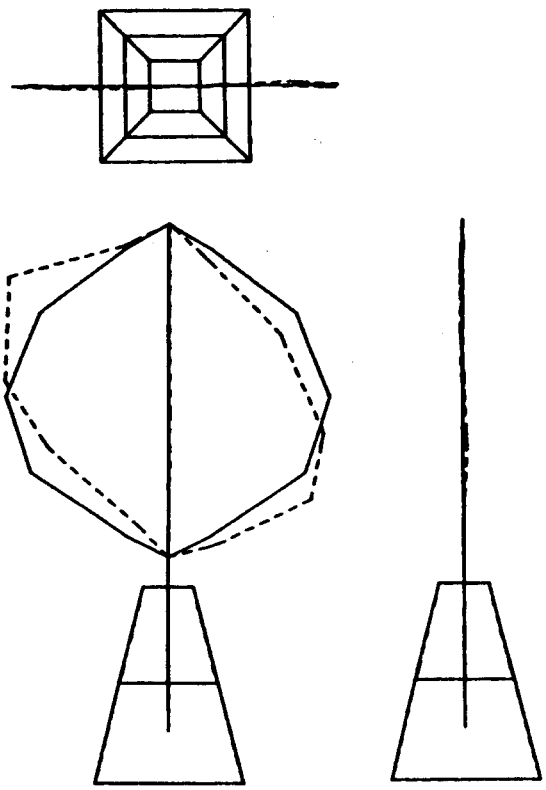

MODE 1: FREQ = 12.3 HZ

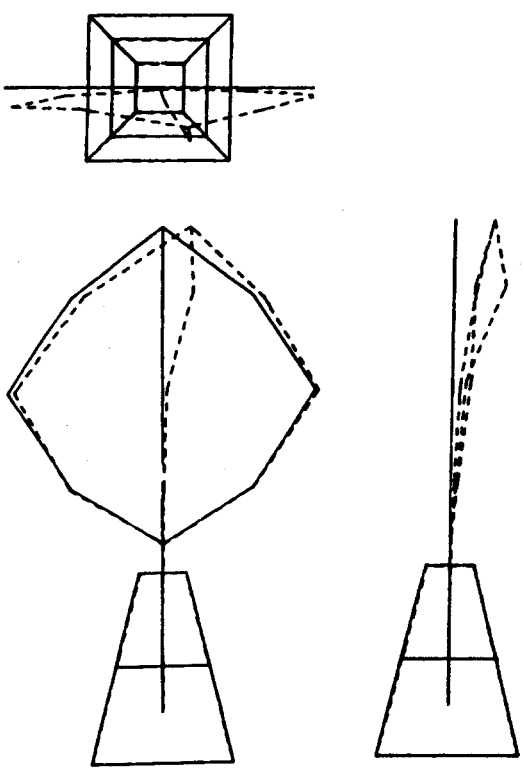

MODE 3: FREQ = 15.3 HZ

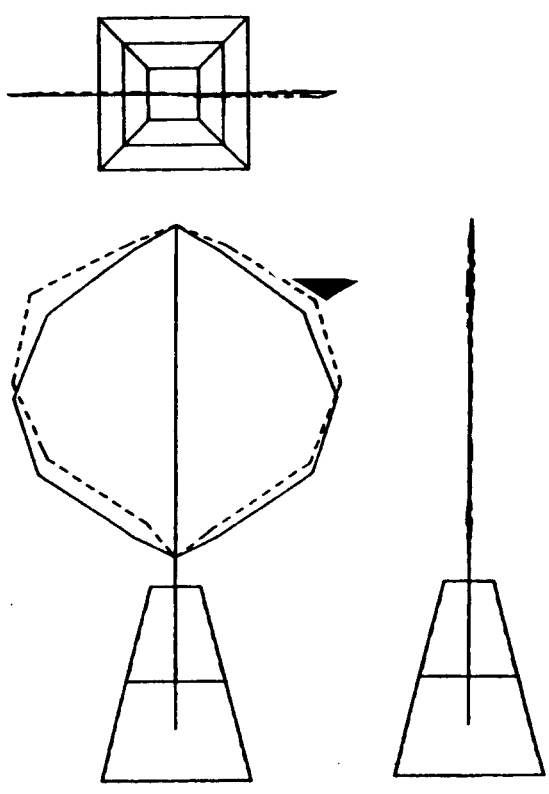

MODE 2: FREQ = 12.5 HZ

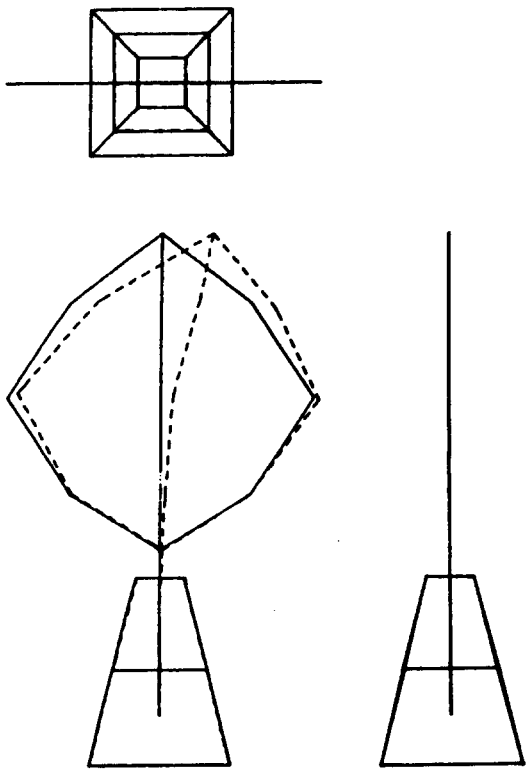

MODE 4: FREQ = 15.8 HZ

Figure 6. Measured Mode Shapes for the Parked 2-m Turbine

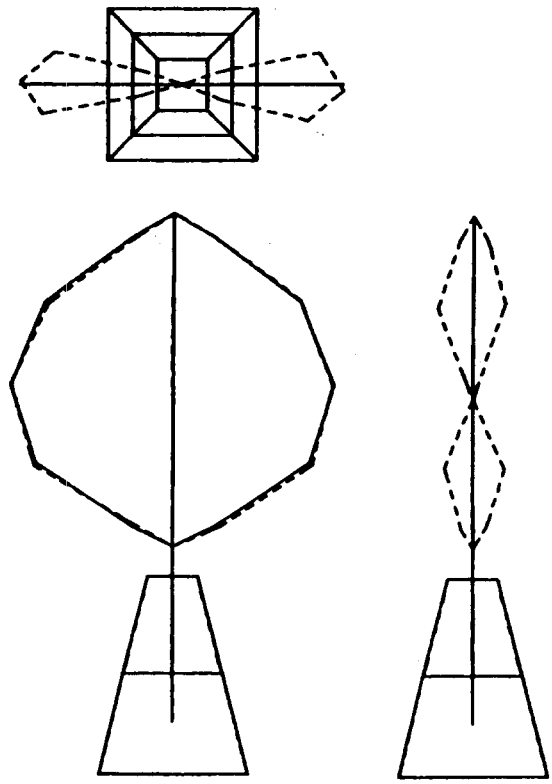

MODE 5: FREQ = 24.4 HZ

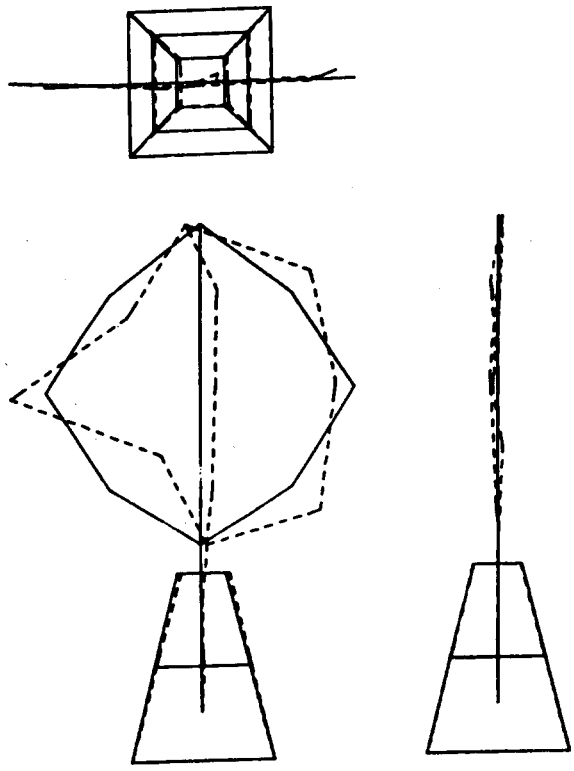

MODE 7: FREQ = 28.3 HZ

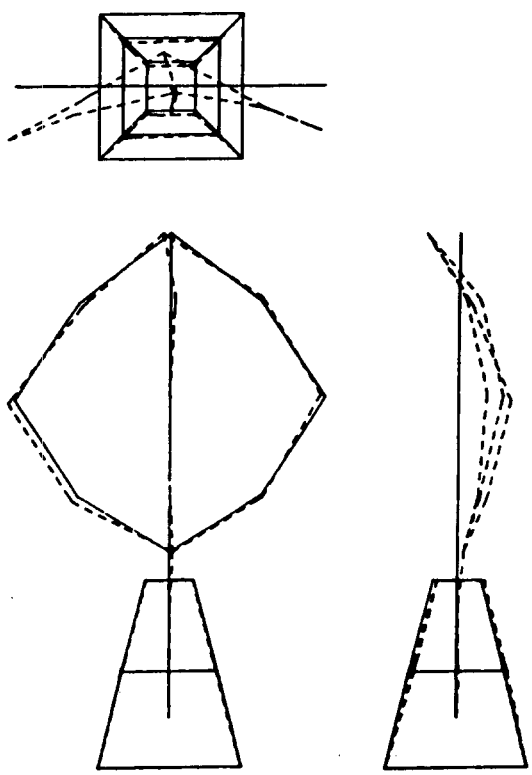

MODE 6: FREQ = 26.2 HZ

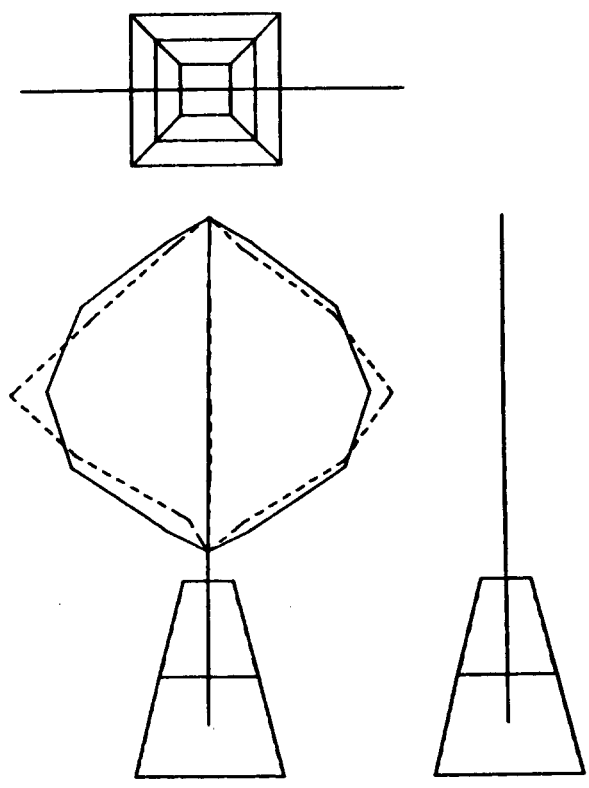

MODE 8: FREQ = 29.7 HZ

Figure 6. (Continued)

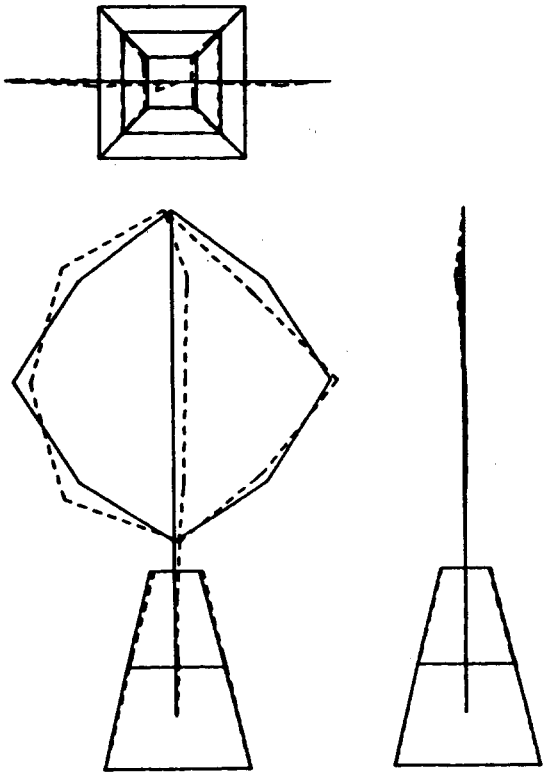

MODE 9: FREQ = 31.5 HZ

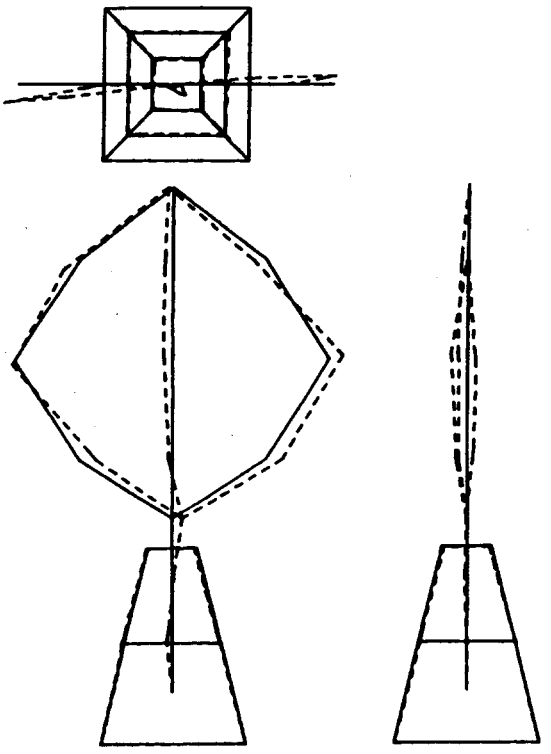

MODE 11: FREQ = 42.0 HZ

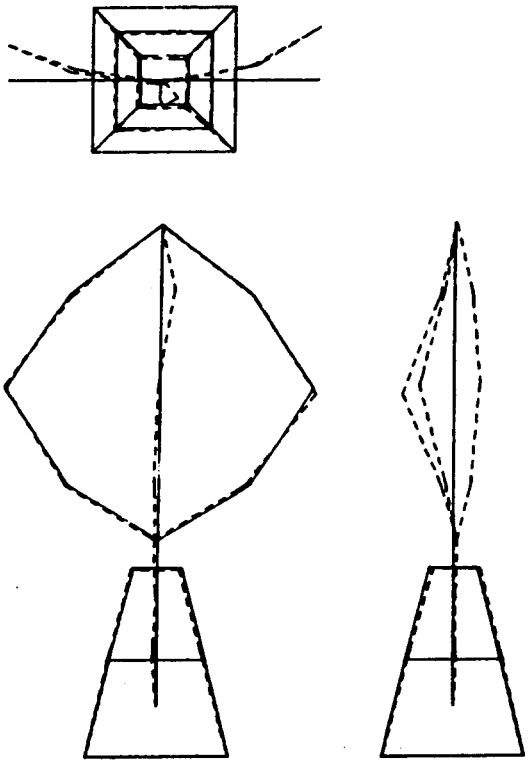

MODE 10: FREQ = 36.5 HZ

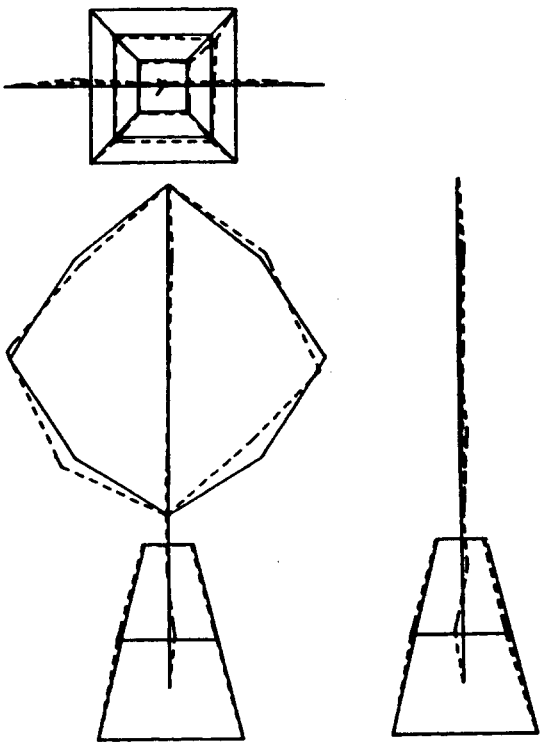

MODE 12: FREQ = 47.7 HZ

Figure 6. (Continued)

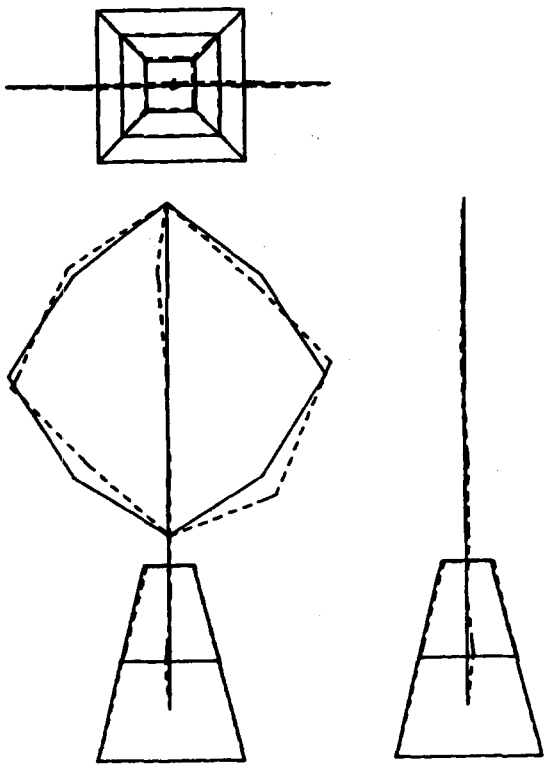

MODE 13: FREQ = 49.1 HZ

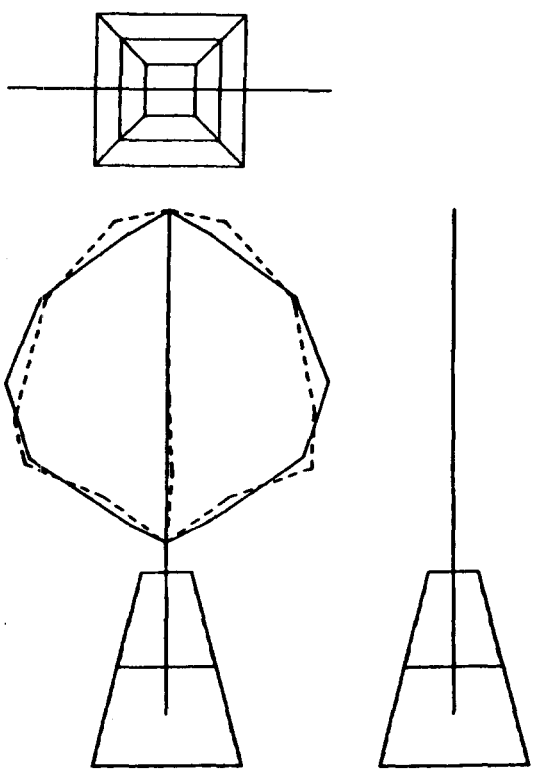

MODE 14: FREQ = 49.5 HZ

Figure 6. (Continued)

Table 2. Parked Frequency Comparison

Mode No.	Measured Modal Frequency (Hz)	Initial Analytical Frequency (Hz)	Modified Analytical Frequency (Hz)
1	12.3	12.5	12.3
2	12.5	12.6	12.4
3	15.3	17.1	15.2
4	15.8	17.2	15.9
5	24.4	22.6	24.4
6	26.2	30.5	26.2
7	28.3	30.6	28.0
8	29.7	30.9	30.6
9	31.5	39.7	31.7
10	36.5	42.3	36.5

Modal Testing of the Rotating Turbine

It was more difficult to obtain frequency response functions from the rotating turbine than from the parked configuration. A proper excitation was the first obstacle to overcome; the collecting of ample response data required for adequate determination of the modes was the second.

The proper excitation device had constraints: (1) the input force should be measured and the excitation should be repeatable; (2) it must excite all the modes of interest; (3) it must not produce secondary hits or banging after being energized; and (4) it must operate at high rotor speeds. In addition, the turbine must be operated in very low winds to reduce aerodynamic input at the discrete frequencies, thus eliminating wind gusting as an excitation source. Since samples should be averaged in order to improve the quality of the frequency response functions, it was important that the samples be similar in excitation location and amplitude level. This constraint tends to eliminate many ideas of throwing or shooting something into the rotating blades as excitation. The excitation must also excite both the rotor and the blade modes. It was observed in the parked test that some of the modes included both blade and tower motion, while others had only one component involved. There was little reason to believe that a shaker attached to the stationary portion of the upper or lower part of the turbine or plucking a guy cable would excite the blade modes.

The technique that was devised for exciting the turbine used a pretensioned cable between the tower and one of the blades. The cable that imposed enforced displacements on both the blade and the tower was suddenly released while the turbine was rotating, thus plucking the turbine. The release device contained a burn wire that was activated remotely at the appropriate operating speed and a force transducer that measured the force applied to the turbine. This excitation technique enjoyed the advantage of modal coupling created by the Coriolis effects so that all of the modes of interest were excited. Fig. 7 shows a diagram of the snap-release device used to excite the turbine while rotating. The cable was adjusted by a turnbuckle located above the quick adjustment come-along, so that after the nylon cord and burn wire were installed, the come-along would put the proper tension on the cable.

For the parked modal, accelerometers were used to measure the response. In the rotating modal test, however, the high steady centrifugal acceleration prevented the use of accelerometers except on the tower. Because strain gages are normally installed on newly designed turbines undergoing initial evaluation (such gages will probably be available on future turbines), the rotating modal test depended primarily on strain gages as response transducers. Strain gages were placed on the blades and tower, using a double active gage in the bridge so that a single axis of bending would be measured. Gages were placed on the leading and trailing edges of the blades to measure edgewise bending, and on inside and outside at maximum blade thickness for flatwise bending. Besides their use in instrumenting the roots of the blades, gages were also installed on the upper and lower tower to read in-plane and out-of-plane bending. Seven of the nine on-board amplifiers boosted the strain signal to 2000 psi/V for all gages to give an adequate level for passing through the slip rings and the long lines to the instrumentation trailer. Because of the projected difficulties in understanding the tower modes, two piezoresistive Endevco 2265-25 accelerometers were placed on the upper tower to record in-plane and out-of-plane motion. These seven strain gages and two accelerometers were wired through the nine on-board amplifiers and to the slip rings.

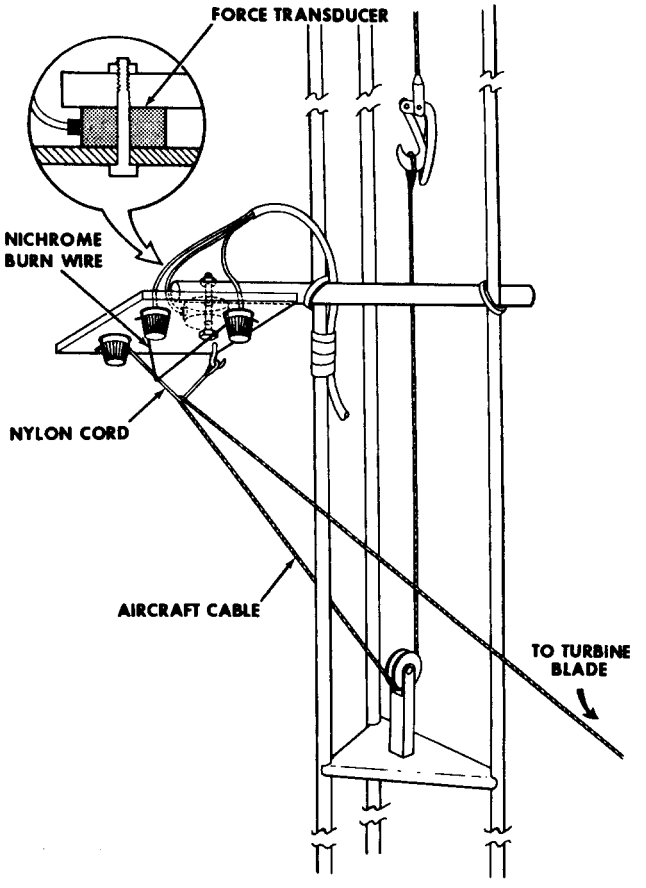

Figure 7. The Snap-Release Device

The performance of the rotating test was fairly straightforward after all the instrumentation had been connected and checked out. The turbine was brought up to the desired speed (100 to 600 rpm) with the electric motor; a remotely controlled power supply provided current through the slip rings to the burn wire; and the preloaded cable was released but still constrained at its ends to prevent random banging. The initial preload gave a dc voltage offset on the force gage; the sudden release caused it to go to zero. When this signal was passed through a high-pass filter, the resulting pulse was typical of the one displayed in Fig. 8. The low-level oscillation prior to the pulse is the three-per-revolution response seen by the force gage resulting from aerodynamic input.

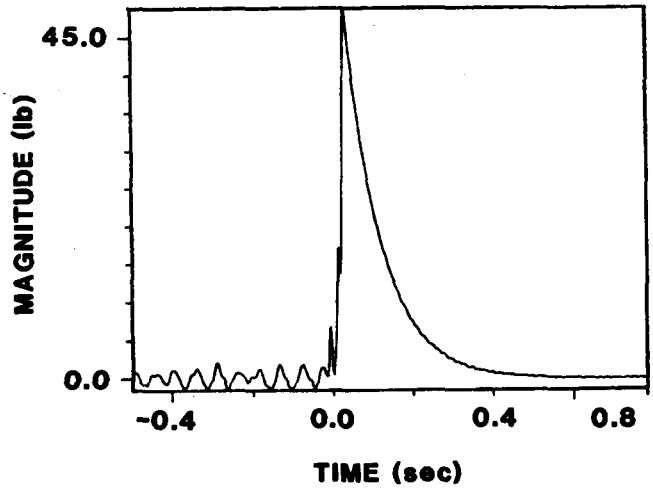

Figure 8. A Typical Filtered Force History Produced by the Snap-Release Device

The high-pass filter used in this test is the ac coupling circuit of a set of amplifiers that amplified the signals before recording them on FM tape. The response signals must also pass through matched filters to avoid relative phase shifts between the response and the excitation. Fig. 9 shows the magnitudes of the frequency response function for the low- and high-pass filters used here, with the 3.0-dB points at approximately 2 and 100 Hz.

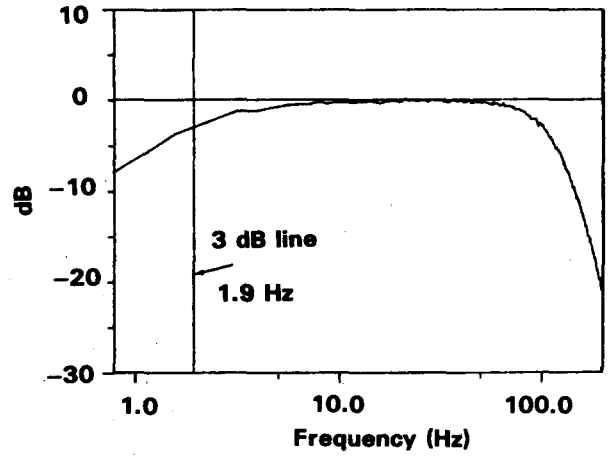

Figure 9. The Magnitude of the Frequency Response Function for the Filter Used in the Rotating Modal Test

Fig. 10 and 11 show typical frequency response functions from the rotating test at 600 rpm. These functions were obtained from data taken by the in-plane and out-of-plane accelerometers located near the top of the tower. Taking into account the scale factors on the two plots, we found that the magnitudes of the two response functions were approximately equal. This indicates that the Coriolis coupling has indeed produced out-of-plane response, even though the initial excitation was strictly in-plane.

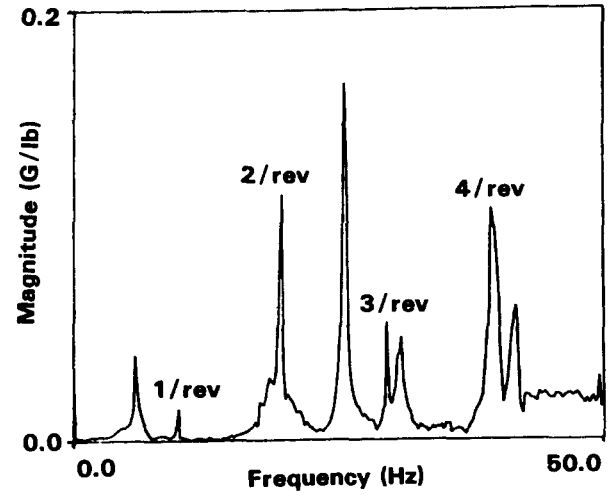

Figure 10. The Frequency Response Function for the In-Plane Tower Accelerometer at a Rotational Speed of 600 rpm

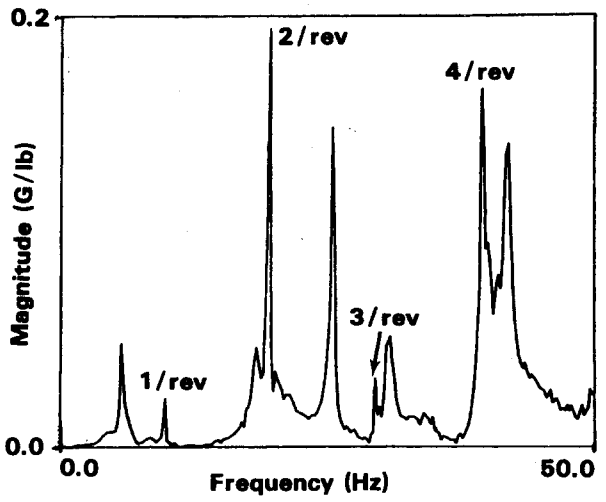

Figure 11. The Frequency Response Function for the Out-of-Plane Tower Accelerometer at a Rotational Speed of 600 rpm

Although the general data quality is represented by that in Fig. 10 and 11, at higher rotational speeds the aerodynamic excitation of the turbine became more prevalent in spite of the low-wind environment. This increase was indicated in the frequency response by the high levels at integral multiples of the rotational frequency.

At each rotational speed, frequency response functions were computed from the data taken with the seven strain gages and the two accelerometers. Ignoring those peaks associated with the aerodynamic excitation, we extracted and tabulated the frequencies of the remaining peaks on each of the response functions. Small variations in the frequency of some of the modes did occur; in those cases an average value was used. Since the mode shapes are complex, magnitude data were used rather than the imaginary component to obtain these modal frequencies.

In view of the small number of transducers on the turbine, a full description of the mode shape is impossible. However, eigenvectors can still be computed with nine components in each vector. One typical eigenvector, corresponding to the second rotor out-of-plane mode and a rotational speed of 300 rpm, is shown below. The magnitude and phase are separated by commas in the vector. The first two components are the accelerations with units of milli-G's, and the last seven are stresses with units of psi.

$$\begin{Bmatrix} \text{tower out-of-plane} \\ \text{tower in-plane} \\ \text{tower out-of-plane} \\ \text{tower in-plane} \\ \text{blade 1, lower edgewise} \\ \text{blade 1, upper edgewise} \\ \text{blade 2, lower edgewise} \\ \text{blade 2, upper edgewise} \\ \text{blade 2, lower flatwise} \end{Bmatrix} = \begin{Bmatrix} 1.00, 90 \\ 1.28, 166 \\ 7.57, 279 \\ 4.25, 178 \\ 1.06, 249 \\ 0.83, 275 \\ 1.12, 256 \\ 0.80, 255 \\ 0.00, --- \end{Bmatrix}$$

This eigenvector has been normalized so that the first component has a unit magnitude and a phase of 90 degrees. Observe the large phase variations that are normally not seen when nonrotating structures are analyzed for their complex modes. The out-of-plane acceleration has a phase of 76 degrees (nearly 90 degrees) greater than the in-plane acceleration. Likewise, the out-of-plane tower strain gage is advanced by 101 degrees over the in-plane gage. The four edgewise strain gages are basically in phase with the out-of-plane deformation of the tower. These phase relationships are caused primarily by rotating coordinate system effects. Structural damping, errors from noise in the initial data, and approximations in the extraction algorithms also contribute. However, from the phase components in the vector, it is clear that the in-plane and out-of-plane motion is approximately 90 degrees out of phase.

The modal frequency versus rpm plot of Fig. 3, generated by finite element analysis, is reproduced in Fig. 12. The experimentally determined modal frequencies from 0 to 600 rpm are superimposed on this figure. The agreement between the predicted and the measured values is excellent, with an average deviation of only 2.2 %. This fine correlation is due in part to the close agreement that existed for the parked modal frequencies. Although the deviation does not appear to be dependent on the rpm, the agreement is not as good at the higher frequencies—generally the case when finite element methods are employed. Another facet of Fig. 12 that should be noted is the occasional jump in the measured frequency from the parked value to the value at 100 rpm. The rather abrupt change in frequency is more prevalent in the higher modes than the lower modes and is probably caused by changing joint interface conditions when the turbine is rotating.

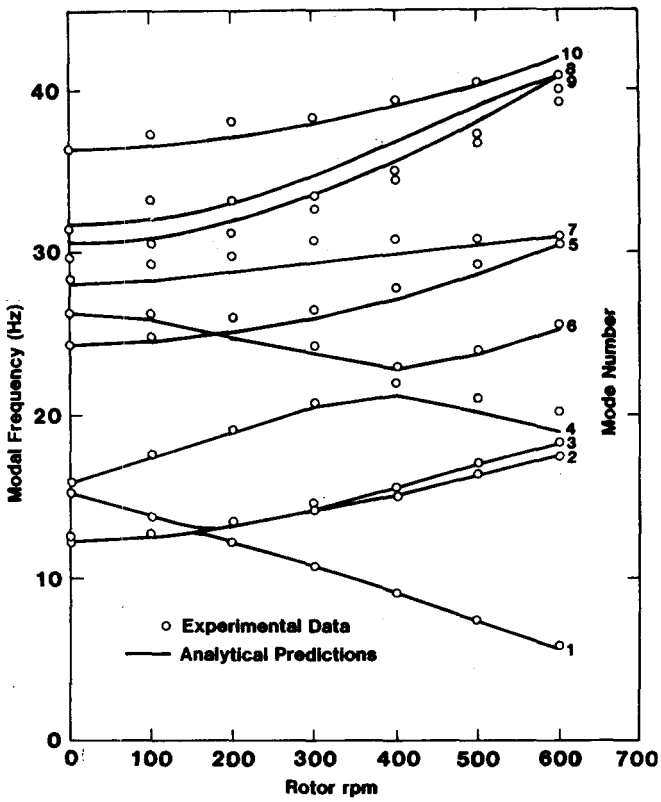

Figure 12. A Comparison of Predicted and Measured Modal Frequencies for the 2-m Turbine as a Function of rpm

Because of the small number of transducers on the turbine, the experimental mode shapes are coarse, and quantitative comparisons to those predicted are difficult. However, as indicated in the theory section, the measure modes are definitely complex rather than real; the in-plane and out-of-plane motions are coupled. These motions are approximately 90 degrees out of phase, consistent with the predicted results.

Modal damping factors were computed at a number of rotational speeds, using minicomputer-based software [21], but it is fairly difficult to compare the damping values for a particular mode shape since the shapes change so drastically with the rotation speed. For example, mode 1 on Fig. 12 is the antisymmetric flatwise mode at 0 rpm. However, that modal degree-of-freedom has a shape that appears to be rotor out-of-plane at 600 rpm, where as the rotor out-of-plane, mode 3, has become more like the antisymmetric flatwise mode. The predominant mode shape associated with a particular modal degree-of-freedom tends to change as the rpm is increased. This modal identification is further complicated by the in-plane and out-of-plane coupling that also exists when the turbine is rotating.

Table 3 tabulates the damping factors and frequencies of the 10 modes shown on Fig. 12 for 0, 300, and 600 rpm. For this table, the modal parameters have been grouped according to a mode shape description rather than to an analytical modal curve as in Fig. 12. This approach may cause some confusion; however, it is the best way to examine trends in the damping factors. Examining the table, observe how the modal damping varies with the rotation speed. In particular, the damping of the first symmetric flatwise and the dumbbell modes steadily declines with increasing rpm, with the damping of the dumbbell mode dropping from 1.8 to 0.16%. The damping of these two modes is particularly important since these are the modes that can cause the turbine to flutter, if the damping becomes negative.

Table 3. Modal Frequencies and Damping Factors for the Rotating Turbine

Mode Description	0 rpm		300 rpm		600 rpm	
	Frequency (Hz)	Damping (% of Critical)	Frequency (Hz)	Damping (% of Critical)	Frequency (Hz)	Damping (% of Critical)
1st antisymmetric flatwise	12.3	1.6	14.8	1.2	18.5	1.8
1st symmetric flatwise	12.5	1.6	14.2	1.4	17.7	0.4
1st rotor out-of-plane	15.3	0.7	10.8	1.7	5.9	2.9
1st rotor in-plane	15.8	0.6	21.0	0.4	25.7	0.3
Dumbbell	24.4	1.8	26.5	0.5	30.7	0.16
2nd rotor out-of-plane	26.2	0.5	24.2	1.0	19.6	0.7
2nd rotor in-plane	28.3	0.5	30.6	1.3	30.9	0.6
2nd symmetric flatwise	29.7	0.5	32.6	2.0	39.2	0.5
2nd antisymmetric flatwise	31.5	0.9	33.8	0.5	40.0	0.9
3rd rotor out-of-plane	36.5	1.1	38.2	1.1	41.4	1.5

Conclusions

A newly developed modal testing technique for a rotating vertical axis wind turbine has been demonstrated. Modal frequencies, damping factors, and mode shape data have been measured on a 2-m turbine. The agreement with frequencies from a finite element prediction is excellent. The mode shape data revealed the complex modes as predicted by the analytical theory. This technique is applicable to large as well as small turbines and, further, can be adapted for use on other rotating systems.

References

[1]T. G. Carne et al, "Finite Element Analysis and Modal Testing of a Rotating Wind Turbine," AIAA Paper 82-0697, *23rd Structures, Structural Dynamics, and Material Conference, Part 2*, New Orleans, May 1982, pp 335-347.

[2]S. V. Hoa, "Vibration of a Rotating Beam With Tip Mass," *J Sound and Vibration* 67(3):369-381 (1979).

[3]P. P. Friedmann and F. Straub, "Application of the Finite Element Method to Rotary Wing Aeroelasticity," *J Am Helicopter Soc* 25:36-44 (January 1980).

[4]D. H. Hodges and M. J. Rutkowski, "Free-Vibration Analysis of Rotating Beams by a Variable-Order Finite-Element Method," *AAIA J* 19:1459-1466 (November 1981).

[5]G. L. Nigh and M. D. Olson, "Finite Element Analysis of Rotating Disks," *J Sound and Vibration* 77(1):61-78 (1981).

[6]J. S. Patel and S. M. Seltzer, "Complex Eigenvalue Solution to a Spinning Skylab Problem," NASA TMX-2378, Vol. II (September 1971).

[7]J. W. Klahs, Jr., and J. H. Ginsberg, "Resonant Excitation of a Spinning, Nutating Plate," *J App Mech* 46:132-138 (March 1979).

[8]W. Warmbrodt and P. Friedmann, "Coupled Rotor/Tower Aeroelastic Analysis of Large Horizontal Axis Wind Turbines," *AIAA J* 18(9):1118-1124 (1980).

[9]W. F. Hunter, "Integrating-Matrix Method for Determining the Natural Vibration Characteristics of Propeller Blades," NASA TN D-6064 (December 1970).

[10]D. J. Ewins and Y. V. K. Sadasiva Rao, "A Theoretical Study of the Damped Forced Vibration Response of Bladed Discs," (Am Soc ME Winter Annual Meeting, 1976).

[11]J. E. Carpenter and E. M. Sullivan, "Structural and Vibrational Characteristics of WADC S-5 Model Propeller Blades," WADC Tech Rpt 56-298, DDC AD 130 787, US Air Force (June 1957).

[12]M. Swaminadham, "Study of the Vibrations of Rotating Blades," Am Soc ME Paper 77-DET-147(1977).

[13]M. Swaminadham et al, "Identification of Resonant Frequencies of Rotating Beams With the Use of PZT Crystals," *Exper Mech*, February 1979, pp 76-80.

[14]D. G. Gorman et al, "Experimental Analysis of Transverse Vibration in Thermally Stressed Rotating Discs," *J Sound and Vibration*, 73(2):221-223 (1980).

[15]E. Möller and U. Ringh, "A Method to Observe and Record Vibration Modes of Rotating Circular Objects," *Exper Mech*, June 1982, pp 226-230.

[16]D. J. Ewins, "An Experimental Investigation of the Forced Vibration of Bladed Discs Due to Aerodynamic Excitation," *Structural Dynamic Aspects of Bladed Disk Assemblies* (New York: Am Soc ME, 1976).

[17]L. I. Walker and F. Kushner, "Experimental Investigation of the Vibratory Characteristics of an Exhaust End Steam Turbine Rotating Blade and Wheel Assembly," Am Soc ME Paper 74-PET-38 (September 1974).

[18]D. U. Noiseux and J. Bêlanger, "Vibration Study of a Vertical Axis Wind Turbine," Institut de recherche de l'hydro-Québec (October 1978).

[19]J. N. Franklin, *Matrix Theory* (Englewood Cliffs, NJ: Prentice-Hall Inc., 1968) p 99.

[20]A. L. Klosterman and R. Zimmerman, "Modal Survey Activity Via Frequency Response Functions," SAE Paper No. 751068, National Aerospace Engineering and Manufacturing Meeting, Culver City, November 1975.

[21]*Modal-Plus Reference Manual,* Version 6 (Milford, OH: The SDRC Corporation 1981).

DISTRIBUTION:

7540 T. Church
7542 D. R. Schafer
7542 T. G. Carne (20)
7542 A. R. Nord

SECOND DISTRIBUTION:

6225 R. H. Braasch - 50